

# Behind armor blunt trauma (BABT) indenter simulating high-velocity impacts from rifle rounds on hard body armor

J. Op 't Eynde<sup>1</sup>, C. P. Eckersley<sup>1</sup>, R. S. Salzar<sup>2</sup>, B. D. Stemper<sup>3</sup>,  
B. S. Shender<sup>4</sup>, T. B. Bentley<sup>5</sup> and C. R. Bass<sup>1</sup>

<sup>1</sup>Duke University; <sup>2</sup>University of Virginia; <sup>3</sup>Marquette University & Medical College of Wisconsin; <sup>4</sup>Naval Air Warfare Center Aircraft Division; <sup>5</sup>Office of Naval Research

## ABSTRACT

*Body armor provides protection against gunshot wounds for both civilian and military personnel. When body armor deforms to defeat an incoming round, the backface deformation of the armor can produce high rate loading of the thorax, injuring the ribcage and internal organs. To improve body armor design without diminishing vital protection or increasing user burden, more accurate thorax impact behavior and injury criteria are needed, which when integrated into finite element models improve their biofidelity. In this study, a repeatable, non-destructive test setup was developed to quantify the effects of behind armor blunt trauma (BABT) in vivo using pigs or other human surrogates. Flash x-ray images of backface deformation in hard body armor provided depth and diameter measurements, which were used to create an indenter machined out of polycarbonate (mass: 0.214 kg, diameter: 100 mm). The indenter with onboard accelerometer was propelled using high pressure helium gas to deliver impacts simulating BABT. Four tests of increasing velocity (22-54 m/s) were performed on two live anesthetized pigs. Thorax impact energy varied from 52 J to 305 J, while indenter acceleration upon impact varied from 3,593 g to 26,656 g. Force was obtained by multiplying indenter mass by acceleration. Displacement during impact was obtained from double integration of the measured acceleration and verified using high speed video images. Rib fractures, liver and lung contusions occurred for all impacts above 126 J, and a 52 J impact caused broken ribs in one pig but not in the other. All rib fractures were non-displaced and did not penetrate the pleura. Observed injuries are similar to reported in-field conditions following BABT. This test methodology provides a repeatable and robust instrumented impact scenario representative of BABT.*

## INTRODUCTION

The benefits of ballistic protective body armor systems have been well characterized for both law enforcement officers and military personnel (Peleg et al., 2006). By reducing the risk of penetrating injury and lowering the energy transferred to the body, it has been estimated that wearing body armor increases the likelihood of survival for law enforcement officers shot in the torso from 32% to 80% (LaTourrette, 2010). Modern body armor can defeat incoming pistol and rifle rounds, trading energy and momentum deposition into the armor for deformation of the armor.

This deformation includes direct deformation of the body armor in soft body armors and deformation with fracture in hard body armors. While protecting the user from penetrating trauma, deformation of the armor backface can cause local, high-rate loading of the underlying tissues resulting in trauma to the thoracic cage and internal organs, leading to serious injuries or even death (Carroll et al., 1978), (Liden et al., 1988), (Cannon, 2001), (Bass et al., 2006). These injuries are often called Behind Armor Blunt Trauma (BABT).

Due to the effectiveness of body armor in protecting the wearer from penetrating gunshot wounds, it is often worn for prolonged periods of time by law enforcement and military personnel. Because of the weight, bulk, and thermal load, it has a negative influence on the physical and psychological performance of the wearer (Shanley et al., 1993), (Ricciardi et al., 2008), (Larsen et al., 2012). Therefore, body armor should be designed to be as light as possible, while still protecting against critical threats. To aid in this design process, balancing weight and protection, computational models with finite element analysis are often used to characterize the injuries caused by BABT. These models are an increasingly important research tool to simulate scenarios that are difficult and costly to test experimentally, and to understand local tissue behaviour. For models to provide valid predictions for injuries and material behaviour, they rely on accurate mechanical properties and dynamics of the biological tissues they represent. A 2012 report by the National Research Council stated that “The fidelity of anatomical, physical, and mathematical finite-element models simulating the human thorax, heart, lungs, liver, and kidneys, is limited” and the presence of “the need for tests using human cadavers and large animal cadavers.” (National Research Council, 2012)

To experimentally characterize BABT, several studies on human cadavers and animal models have been performed. Early studies on live goats with soft body armor established an injury threshold based on projectile velocity, with the notable injuries being in the lungs and ventricles when the impact was near the heart (Montanarelli et al., 1973), (Goldfarb et al., 1975), (Carroll et al., 1978). Later studies on pigs also indicated severe pulmonary injuries for high-energy impacts with soft body armor (Liden et al., 1988). More recent studies evaluating hard body armor in pigs (Sarron et al., 2000), (Gryth et al., 2007), (Sondén et al., 2009) and human cadavers (Bass et al., 2006) have found similar injury patterns. While these studies provide valuable descriptions of the physiological effect of BABT and an injury estimate in one specific condition, injury criteria for BABT are limited to the costal and sternal fracture criteria presented in (Bass et al., 2006). High morbidity in BABT results from damage to the lung, heart, and liver (Mirzeabasov et al., 2000), (Cannon, 2001), (Drobin et al., 2007), (Gryth et al., 2007), but injury criteria for these soft tissues have not been developed. Current criteria for assessing BABT risk rely on studies determining backface deformation in clay or ballistic gelatin; neither have direct correlation to human or animal models and are insufficient for developing accurate thoracic BABT injury criteria (Gryth et al., 2007), (Hanlon et al., 2012). Development of injury criteria for soft tissues will aid in future body armor assessment and design.

In this study, a repeatable, non-destructive test setup was developed to quantify the effects of behind armor blunt trauma (BABT) in vivo using pigs or other human surrogates. The setup using an indenter will allow us to obtain thorax dynamics, thorax material properties, and determine injury risk curves for rib fractures, bruising, and soft tissue injuries in future studies.

## METHODS

### Indenter Development

From previous studies (Sarron et al., 2000), (Bass et al., 2006), flash x-ray images provided depth and diameter measurements of maximum backface deformation in hard body armor during rifle round impact with areal densities appropriate for hard body armor. These measurements were used as the model to create an indenter machined out of a polycarbonate material with a mass of 0.214 kg, a diameter of 100 mm, and a dome height of 25 mm. An accelerometer (Endevco 7270) and battery powered data acquisition system (Slice Nano, DTS) were secured inside the indenter, in order to record the acceleration without having any external attachments. A back panel sealed off the indenter and provided flight stability with carbon fibre fins.

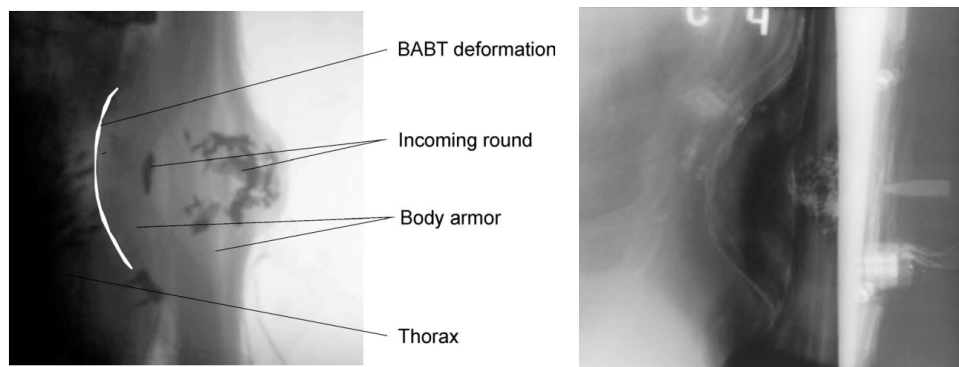


Figure 1: Maximum backface deformation profile in hard body armor from (a) Bass et al., 2006 (Bass et al., 2006) and (b) Sarron et al., 2000 (Sarron et al., 2000).

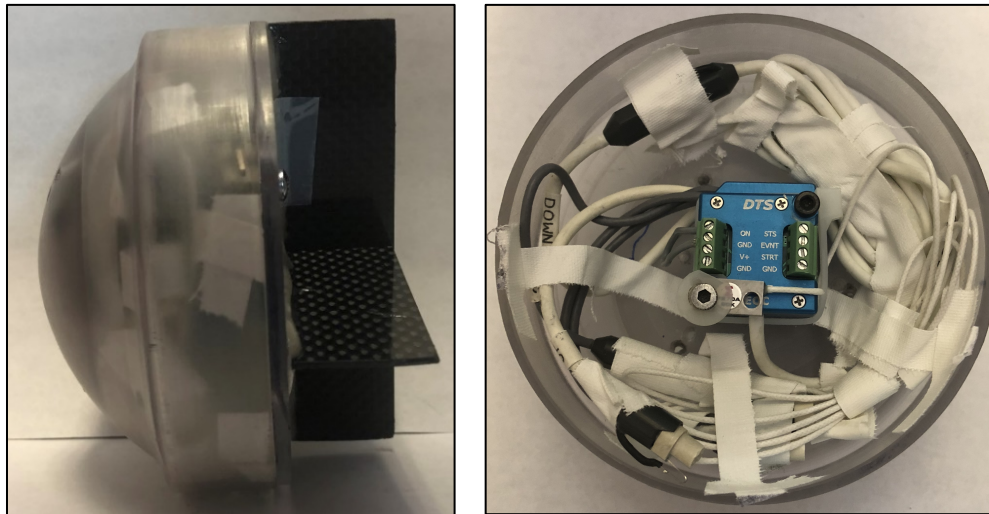


Figure 2: Polycarbonate indenter design with onboard accelerometer and data acquisition.

## Impact tests

To achieve a high-speed simulated BABT, the indenter was loaded into a tightly fitted tube. The release of pressurized helium gas propelled the indenter to the target, placed at the end of the tube. Four tests of increasing velocity (22-54 m/s) were performed on each of two live anesthetized pigs, impacting the upper thorax and the lower thorax bilaterally. The two Yorkshire pigs were approximately six months old pigs with a mass of 38.9 kg and 38.3 kg. Velocities were chosen such that the kinetic energy of the indenter corresponded to realistic impact energy from a rifle round. A previous study (Arborelius et al., 2012) found that kinetic energy of the indenter in BABT simulation experiments most closely correlated with injury severity. The impact sites were situated above approximately the 5th and 9th rib of the animal, to achieve unobstructed impacts superficial to the lungs and liver. The animal was positioned prone with front legs forward on a lift table which was repositioned to place the desired impact site in line with the indenter (Figure 3). All procedures on these animals were approved by the Duke University Institutional Animal Care and Use Committee (IACUC). The animals were ventilated and vital signs were monitored during testing. After each impact, a 30-minute waiting period was allowed to ensure vital signs returned to a stable condition. Impacts were recorded with a high-speed video camera (Phantom V711, Vision Research) at 7500 frames per second.

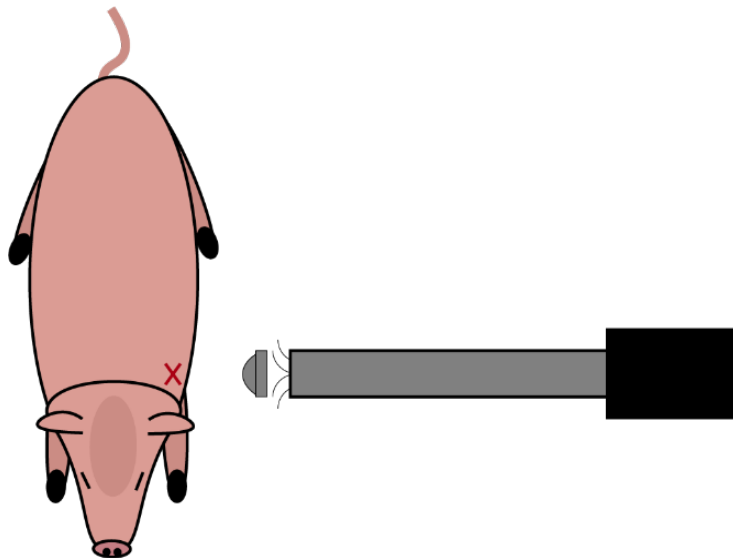


Figure 3: Test setup with pig, indenter, and launch tube.

## Data Analysis

Indenter acceleration was recorded at 100 kHz sample frequency. Force was obtained by multiplying indenter mass by acceleration. Velocity was obtained by integrating the measured acceleration over time, and displacement during impact was obtained by integrating that velocity signal. Flight velocity was verified by high speed video analysis and matched closely the velocity



obtained by integration ( $<1\%$  error). Force-displacement behaviour was visualized for each impact. The impact stiffness was calculated as the steepest slope of the force displacement curve during the loading phase of the impact.

## Injury assessments

After each test, the impact location was palpitated to identify any displaced rib fractures. Significant bruising at the impact location was observed and photographed. Thirty minutes after the last impact, the animal was sacrificed, and a necropsy was performed. Injuries to ribcage and thorax organs were assessed and photographed during necropsy and micro-CT scans were taken of the lungs, liver, and ribcage.

## RESULTS

All four impacts were performed on each animal with a 30-minute waiting time in between. Vitals returned to a stable condition after each impact, however, there were short periods of cardiovascular instability following the two highest intensity impacts on animal #1. A time history for the heart rate and blood oxygen saturation for animal #2 is shown in Figure 6.

The results from the accelerometer data are shown in Table 1. Impact energy varied from 52 J to 306 J, by changing the incoming indenter speed from 22 m/s to 54 m/s. The peak acceleration of the indenter on impact ranged from 4,856 g to 26,656 g, resulting in a peak impact force from 7.5 kN to 55.7 kN. An example of the force-displacement curve and acceleration time history is shown in figure 4. The impact stiffness (slope of the curve) for this example is 24.6 kN/mm.

Table 1: Impact tests metrics

Animal Number	Velocity [m/s]	Energy [J]	Peak Impact Acceleration [g]	Peak Impact Force [kN]	Stiffness [kN/mm]
1	22.2	52.5	4,856	10.1	16.4
	36.9	145.1	11,283	23.6	24.6
	47.0	235.2	18,596	38.9	31.4
	53.6	305.5	26,656	55.7	36.6
2	23.1	56.6	3,593	7.5	11.0
	34.5	126.8	7,030	14.7	14.1
	37.2	147.4	7,019	14.7	15.1
	39.5	166.3	12,134	25.4	24.2

Each animal received an impact at four different locations on the thorax. All impacts were performed in order from low velocity to high velocity.

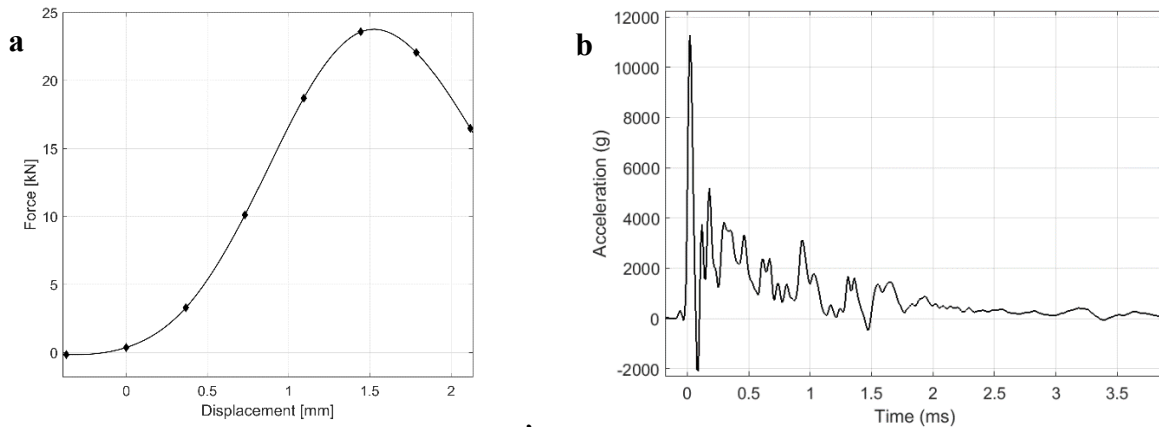


Figure 4: (a) Force-displacement graph of the initial interaction of the indenter with the thorax, smoothed using cubic spline interpolation. Measured datapoints are indicated by the markers. (b) Acceleration-time history of the same 145 J impact, unprocessed. Time = 0 was aligned with a sharp increase in acceleration experienced upon first interaction of the nose of the indenter with the thorax during impact.

Extensive bruising of the impact location occurred for each impact, similar to bruising seen in in-field BAPT, but the skin remained intact. An example of the bruising can be seen in Figure 5. No rib fractures were seen for the lowest intensity test for animal #1, but a single broken rib was found under the impact site of the low intensity impact for animal #2, which was not detected before necropsy. At all other impact locations, multiple, non-displaced rib fractures were found. The impacts caused damage to the underlying internal organs. Serious lung contusions were found underneath the impact site of all but the lowest intensity impacts for both animals, and the lung exposed to 235 J and 305 J impacts was nearly entirely filled with blood. Micro CT sections of the lungs from animal #2 are shown in Figure 7. The liver of both animals, which was situated directly under the respective 145 J and 147 J impact sites, suffered contusions and lacerations, as seen in Figure 8. Following the two high intensity impacts for animal #1, there was a short period of rapid forceful muscle twitches in the impact area.



Figure 5: Bruising following 235 J (left) and 305 J (right) impacts on animal #1.

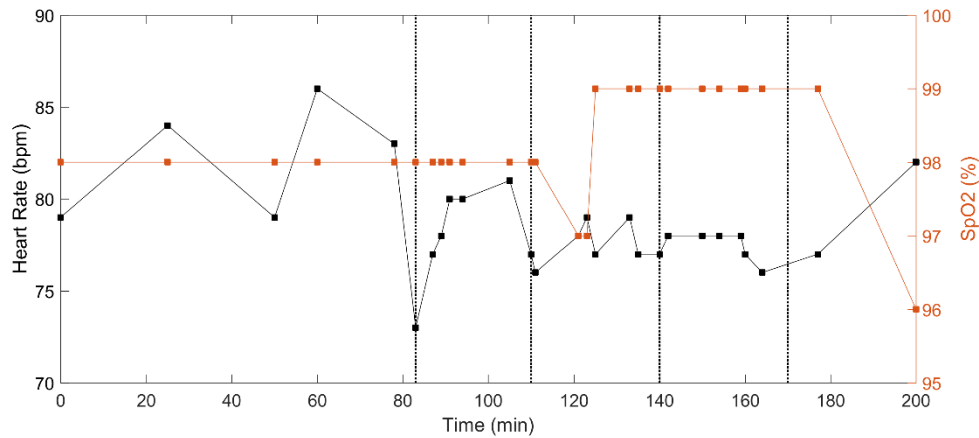


Figure 6: Heart rate and blood oxygen saturation (SpO<sub>2</sub>) for animal #2. The dotted vertical lines indicate the four impacts.

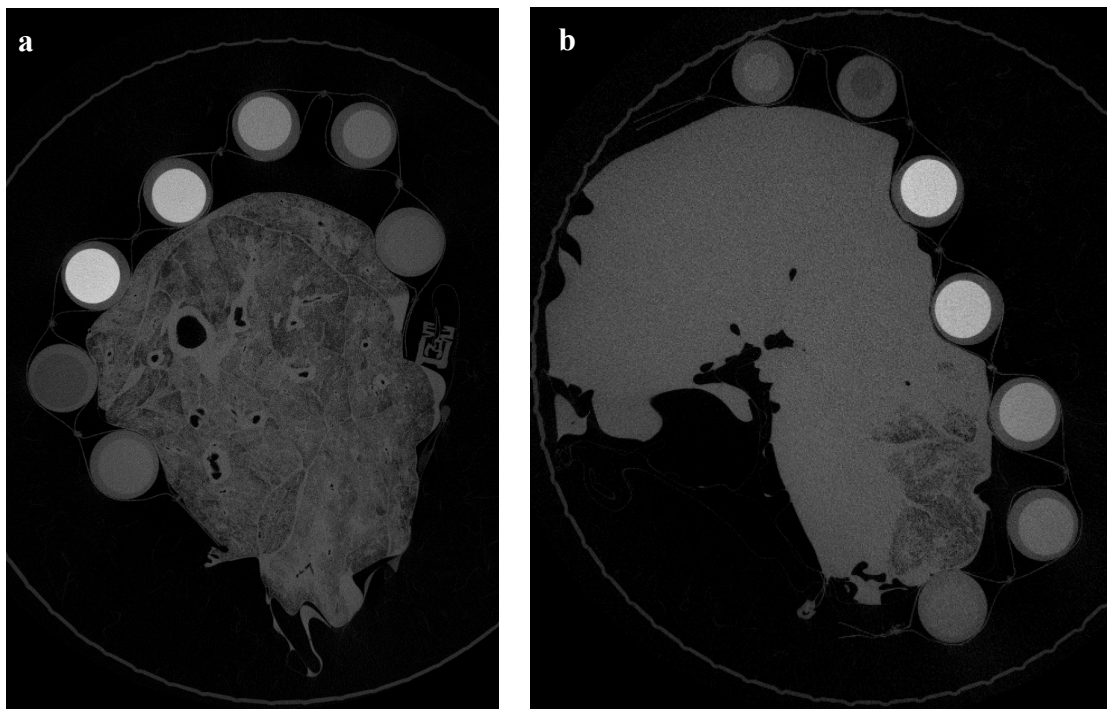


Figure 7: Blood (light grey) in between alveoli (fine, dark grey structures) of two lungs from animal #2 as seen on Micro CT scans. (a) is a slice of the right lung under the low intensity impact site and shows small areas of bleeding in an otherwise functioning lung. In (b), a section of the left lung is shown, which was exposed to two impacts at higher intensity. The majority of the alveoli in this section are filled with blood, indicating serious injury. The circles present in the scan are part of a CT phantom, included as calibration for the density of scanned materials.

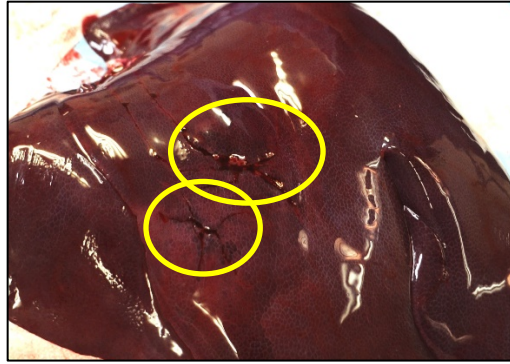


Figure 8: Liver of animal #2 after necropsy. Two lacerations on the parenchyma are examples of BABT.

## DISCUSSION

The impact metrics measured during these tests are representative of a realistic BABT injury scenario. Bass et al. (2006) measured peak impact forces in the 15k-30kN range on a cadaver sternum behind a hard body armor for a 7.62 mm round. They calculated a 50 % risk of sternum fracture at 24.9 kN. Injury severity in the current study matched expectations based on a previous indenter study (Arborelius et al., 2012), as they reported an approximate impact energy threshold of 210 J for the transition from moderate to severe injuries. Park et al. (2012) concluded that the transferred kinetic energy to clay from a 9 mm round impact on soft body armor was 48-100 J, and for a .44 Magnum it was 177 J. The amount of transferred energy was estimated to be 6-13% the energy of the incoming round. While no such estimates have been made for hard body armor, the results presented in this paper encompass these energy levels relevant for BABT injuries. In addition to that, the injuries observed in the animals also correspond to realistic injuries seen in modern military combat. The injuries sustained during BABT, as seen in this study, while not fatal, can be life threatening if medical treatment is not immediately available. When they are treated, they can still cause prolonged morbidity for the soldier.

In this study, only two animals were used, and four impacts were performed on each animal. While the structure of the ribcage stayed intact, fractured ribs under one impact site might have affected the integrity of the ribcage for an adjacent impact site. This is one of the limitations of the study.

The muscle twitch in the chest wall of the pig following the high-velocity impacts could be due to a reflex or local nerve damage. This behaviour is not well documented, and the response needs to be further investigated. If the behaviour is consistent, surface electromyogram electrodes could have potential as a mechanism to alert for possible BABT in military combat scenarios, where access to medical scanning equipment for evaluating these injuries might be challenging.

Future work could include expanded test conditions to allow us to find injury thresholds for the thoracic organs and develop an injury criterion. Injury criteria for these soft tissues will be instrumental in developing meaningful standards for body armor performance. In addition to

BABT simulations impacting the ribcage for a whole thorax response, the impacts can be delivered directly to the organs to evaluate organ level injury criteria and mechanical behaviour. This data would be invaluable for the development of finite element models of BABT and aid in the design of new body armor.

## CONCLUSIONS

A novel experimental method was developed to test the effects of behind armor blunt trauma (BABT) non-destructively. The use of an indenter created based on armor backface deformation allows for a controlled test design. The pig animal model suffered serious injuries similar to in-field reported conditions and previous experimental and theoretical studies. Rib fractures, contusions and bleeding in the lung, and liver contusions and lacerations were observed. Thorax and indenter mechanics upon impact were recorded in great detail. This test methodology provides a robust instrumented impact scenario representative of BABT.

## ACKNOWLEDGEMENTS

The authors gratefully acknowledge the funding and collaboration from MTEC-18-04-I-PREDICT-07, Incapacitation Prediction for Readiness in Expeditionary Domains, an Integrated Computational Tool (I-PREDICT) Thorax Model Prototype.

## REFERENCES

- ARBORELIUS, U., TYRBERG, A., GUSTAVSSON, J., MALM, E., GRYTH, D., OLSSON, L., SKOGLUND, M., ROCKSÉN, D. (2012). Physiological Effects in Pig, and Mechanical Response in an Armour Test Rig, to Graded Chest Impacts using a Behind Armour Blunt Trauma (BABT) Simulator. Personal Armour Systems Symposium, Nuremberg, Germany.
- BASS, C. R., SALZAR, R. S., LUCAS, S. R., DAVIS, M., DONNELLAN, L., FOLK, B., SANDERSON, E., WACLAWIK, S. (2006). Injury risk in behind armor blunt thoracic trauma. *International Journal of Occupational Safety and Ergonomics*, 12(4): 429–442.
- CANNON, L. (2001). Behind armour blunt trauma-an emerging problem. *Journal of the Royal Army Medical Corps*, 147(1): 87-96.
- CARROLL, A. W., SODERSTROM, C. A. (1978). A new nonpenetrating ballistic injury. *Annals of Surgery*, 188(6): 753.

DROBIN, D., GRYTH, D., PERSSON, J. K., ROCKSÉN, D., ARBORELIUS, U. P., OLSSON, L.-G., BURSELL, J., KJELLSTRÖM, B. T. (2007). Electroencephalogram, circulation, and lung function after high-velocity behind armor blunt trauma. *Journal of Trauma and Acute Care Surgery*, 63(2): 405-413.

GOLDFARB, M. A., CIUREJ, T. F., WEINSTEIN, M. A., METKER, L. W. (1975). A method for soft body armor evaluation: medical assessment. National Technical Information Service. Springfield, VA, USA.

GRYTH, D., ROCKSÉN, D., PERSSON, J. K., ARBORELIUS, U. P., DROBIN, D., BURSELL, J., OLSSON, L.-G., KJELLSTRÖM, T. B. (2007). Severe lung contusion and death after high-velocity behind-armor blunt trauma: relation to protection level. *Military Medicine*, 172(10): 1110-1116.

HANLON, E., GILLICH, P. (2012). Origin of the 44-mm behind-armor blunt trauma standard. *Military Medicine*, 177(3): 333–339.

LARSEN, B., NETTO, K., SKOVLI, D., VINCS, K., VU, S., AISBETT, B. (2012). Body armor, performance, and physiology during repeated high-intensity work tasks. *Military Medicine*, 177(11): 1308-1315.

LATOURETTE, T. (2010). The life-saving effectiveness of body armor for police officers. *Journal of Occupational and Environmental Hygiene*, 7(10): 557–562.

LIDEN, E., BERLIN, R., JANZON, B., SCHANTZ, B., SEEMAN, T. (1988). Some observations relating to behind-body armour blunt trauma effects caused by ballistic impact. *The Journal of trauma*, 28(1 Suppl): S145-148.

MIRZEABASOV, T., BELOV, D., TYURIN, M., KLYAUS, I. (2000). Further investigation of modelling system for bullet-proof vests. *Personal armour systems symposium*.

MONTANARELLI, N., HAWKINS, C. E., GOLDFARB, M. A., CIUREJ, T. F. (1973). Protective garments for public officials. ARMY LAND WARFARE LAB ABERDEEN PROVING GROUND MD.

NATIONAL RESEARCH COUNCIL (2012). Testing of body armor materials: Phase III. National Academies Press. Washinton, DC, USA.

PARK, J., CHI, Y., HAHN, M., KANG, T. (2012). Kinetic dissipation in ballistic tests of soft body armors. *Experimental mechanics*, 52(8): 1239-1250.

PELEG, K., RIVKIND, A., AHARONSON-DANIEL, L., ISRAELI TRAUMA GROUP (2006). Does body armor protect from firearm injuries? *Journal of the American College of Surgeons*, 202(4): 643–648.

RICCIARDI, R., DEUSTER, P. A., TALBOT, L. A. (2008). Metabolic demands of body armor on physical performance in simulated conditions. *Military Medicine*, 173(9): 817-824.

SARRON, J., DESTOMBE, C., GØTSE, H., MAYORGA, M. (2000). Physiological results of NATO BABT experiments. Personal Armour Systems Symposium, Colchester, UK.

SHANLEY, L. A., SLATEN, B. L., SHANLEY, P. S. (1993). Military protective clothing: Implications for clothing and textiles curriculum and research. Clothing and Textiles Research Journal, 11(3): 55-59.

SONDÉN, A., ROCKSÉN, D., RIDDEZ, L., DAVIDSSON, J., PERSSON, J. K., GRYTH, D., BURSELL, J., ARBORELIUS, U. P. (2009). Trauma attenuating backing improves protection against behind armor blunt trauma. Journal of Trauma and Acute Care Surgery, 67(6): 1191-1199.